



Urban land use carbon emission intensity in China under the “double carbon” targets: spatiotemporal patterns and evolution trend

Nan Ke¹ · Xinhai Lu¹ · Xupeng Zhang² · Bing Kuang³ · Yanwei Zhang¹

Received: 14 June 2022 / Accepted: 22 September 2022 / Published online: 8 October 2022
© The Author(s), under exclusive licence to Springer-Verlag GmbH Germany, part of Springer Nature 2022

Abstract

In-depth research on the spatiotemporal patterns and evolution trend of urban land use carbon emission intensity (ULUCEI) can reveal the internal relationship between urban land use and carbon emissions, which is crucial for achieving carbon emission reduction and “double carbon” targets. This paper proposed a conceptual framework of ULUCEI; the methods of kernel density estimation (KDE), exploratory spatial data analysis (ESDA), and spatial Markov chains were adopted for exploring the spatiotemporal patterns and evolution trend of China’s ULUCEI from 2000 to 2017. The following conclusions are drawn through research. (1) There was an increasing trend in ULUCEI in China from 0.102 in 2000 to 0.283 in 2017. From the regional perspective, the ULUCEI in the eastern region is markedly higher than that in the central and western regions. Moreover, the results of nuclear density estimation indicate that China’s ULUCEI shows an obvious upward and polarized trend. (2) China’s ULUCEI shows a positive spatial autocorrelation. The types of spatial agglomeration include “high-high” agglomeration, “high-low” polarization, “low-high” collapse, and “low-low” homogeneity, and there are obvious disparities in the distribution rules of cities with different spatial agglomeration forms. (3) China’s ULUCEI presents strong stability and “club convergence” trend. Moreover, spatial factors significantly affect the dynamic transition of China’s ULUCEI, and its effect on the shifting upwards gradually enhances with increasing lag type. This paper therefore suggests that policymakers should formulate differentiated urban land low-carbon use models and carbon emission reduction policies to reduce ULUCEI.

Keywords Carbon emission intensity · Urban land use · Spatiotemporal patterns · Evolution trend · Double carbon targets · China

Introduction

Carbon emissions generated by burning fossil fuels have seriously threatened global climate stability and sustainable human development (Schoor et al. 2015; Tollefson 2016; Cramer et al. 2018; Yang et al. 2021). Under the severe

situation of global climate issues, carbon emission reduction has gradually become a consensus in the world (Wang et al. 2019a; Andiappan et al. 2019; Chen et al. 2022a). For a long time, developing countries have faced the dilemma of balancing economic growth and carbon emissions, posing a huge challenge to global carbon emission reduction (Xu and Yang 2019; Jin et al. 2020; Baloch et al. 2021; Wang et al. 2021a). As the largest developing country around the world, China has become the largest carbon emitter in 2007 (Dong et al. 2013; Wang et al. 2021a). Notably, China’s carbon emissions reached 10.67 Gt in 2020, accounting for about 30.65% of global carbon emissions (Ritchie et al. 2020). To address global climate issues, China has taken an active part in global climate governance, proposing the ambitious “double carbon” targets of carbon peaking by 2030 and carbon neutrality by 2060 (Normile 2020; Wang et al. 2021a).

As the concentration areas of socio-economic activities, urban areas cover less than 3% of the global land areas, consume more than 66% of the global energy, and generate more

Responsible Editor: V.V.S.S. Sarma

✉ Xinhai Lu
xinhailu@163.com

✉ Xupeng Zhang
zhangxupeng@cug.edu.cn

¹ College of Public Administration, Huazhong University of Science and Technology, Wuhan 430074, China

² School of Public Administration, China University of Geosciences, Wuhan 430074, China

³ College of Public Administration, Central China Normal University, Wuhan 430079, China

than 70% of the world's carbon emissions (Grimm et al. 2008; Romero-Lankao et al. 2014). In this case, urban areas play a key role in seeking solutions and mitigation strategies for global climate change issues (Ribeiro et al. 2019; Wang et al. 2021b; Chen et al. 2022b). More importantly, urban land utilization is not only closely related to urban energy consumption and industrial activities (Carpio et al. 2021; Zhang et al. 2022), but also carries the carbon emission intensity at the urban spatial scale (Wang et al. 2021b). Compared with total carbon emissions or per capita carbon emissions, it is more practical to reduce carbon emission intensity to promote carbon emission reduction (Jotzo and Pezzey 2007). In order to explore the internal mechanism between urban land use system and carbon emission system, this paper proposes a conceptual framework of urban land use carbon emission intensity (ULUCEI).

The concept of ULUCEI is developed on the basis of "urban land use intensity." The biggest difference between them is that ULUCEI reflects the carrying pressure of carbon emissions on urban land areas (Huang et al. 2013; Cui et al. 2019), focusing on the coordinated development of urban land use system and carbon emission system, while urban land use intensity emphasizes the coupling between economic development and urban land areas (Kuang et al. 2020a). Undoubtedly, the higher value of ULUCEI means that per unit of urban land carries more carbon emissions. Reducing ULUCEI within the limited urban space is helpful for promoting urban carbon emission reduction under the "double carbon" targets. Therefore, exploring the spatiotemporal patterns and evolution trend of China's ULUCEI can contribute to reveal the internal relationship between urban land use and carbon emissions, which is of great practical significance for formulating reasonable urban carbon reduction strategies, exploring low-carbon urban development models, and achieving the "double carbon" targets.

The remainder of this paper is organized as follows. "Literature review" reviews the literature of relevant studies on ULUCEI. "Methods and data" presents the research methods and data in this paper. "Results and discussion" analyzes the spatiotemporal patterns and evolution trend of ULUCEI in China from 2000 to 2017. "Conclusions and policy implications" gives the conclusions and provides some policy implications.

Literature review

Relevant studies on ULUCEI have focused on the following three aspects, which are the impact of land use/cover change (LUCC) on carbon emissions, the association between land use and carbon balance, and the inner relationship between urban land use and carbon emissions. LUCC caused by human activities is a major source of carbon emissions and

an important driver of global climate change (Mendelsohn and Sohngen 2019; Simmonds et al. 2021; Tang et al. 2021). Exploring the carbon emissions from LUCC is a key way to gain insight into the impact of human activities on regional sustainability. Therefore, the impact of LUCC on carbon emissions has gradually attracted the attention of scholars and policymakers. Studies on the impact mechanism of LUCC on regional carbon emissions show that carbon emissions continue to increase in the process of LUCC (Zhu et al. 2019; Zhang et al. 2022), and the increased carbon emissions are mainly concentrated in urban central areas (He and Zhang 2022; Zhang et al. 2022). There are also studies focused on the role of urban spatial form in reducing carbon emissions (Liu et al. 2020; Wang et al. 2020). Some scholars believe that the small-scale, compact, and dense urban land space patterns can produce less carbon emissions (Wang et al. 2019b, 2020), and should effectively control urban land sprawl to achieve low-carbon urban development (Xia et al. 2019).

Land utilization not only changes the carbon sequestration in land ecosystems (Bordoloi et al. 2022), but also alters carbon emissions in the intensive areas of human activities (Tian et al. 2021), thereby significantly affecting the global carbon balance (Neupane et al. 2017). Research on the relationship between land use and carbon balance has been proliferating in recent years (Cui et al. 2019; Huang et al. 2020; Tong et al. 2020). Integrating land use dynamics and carbon balance into the urban management system, the impact of land use on the carbon balance indicated that the carbon balance rate showed a sharp downward trend in the Beijing-Tianjin-Hebei region from 2000 to 2015 (Wang et al. 2021c). In addition, the natural land use type exhibited competition relationships in the urban fringe areas, and exacerbated the local carbon imbalance (Xia and Chen 2020). Actually, scholars mainly evaluate the carbon balance changes caused by land utilization through carbon sources and carbon sinks (Huang et al. 2020; Tong et al. 2020). Studies of urban land use conversion rates affecting carbon balance find that the increase in construction land and decrease in vegetation coverage directly caused a significant decline in carbon storage (Zhu et al. 2019; Chuai et al. 2019; Feng et al. 2020). Especially in megacities and urban agglomerations, urban expansion leads to higher depletion of carbon storage (Chuai et al. 2015a; Liu et al. 2019).

For a long time, scholars have been highly concerned about the relationship between urban land use and carbon emissions (Fang et al. 2015; Wang et al. 2016; Zhang et al. 2018; Xia et al. 2020; Wu et al. 2022). Human activities can influence regional carbon emissions by changing land use patterns (Ou et al. 2013; Li et al. 2018). Related studies consider carbon emissions of urban construction land utilization as the main contributors of urban carbon emissions (Chuai et al. 2015b; Ali et al. 2018; Wang et al. 2019c; Zhang et al.

2022). Optimizing urban land use structure plays a key role in carbon reduction and is an important policy tool worthy of adoption by land managers and policymakers (Cen et al. 2015; Chuai et al. 2015b, 2016; Tang and Hu 2021). Due to the fact that the type of urban industrial activities directly affects the carbon emission effect of urban land, rational configuration of urban land resources is an important way to promote carbon emission reduction (Shu and Xiong 2019). Moreover, carbon emissions have gradually become an obvious obstacle to the realization of intensive urban land utilization (Wang et al. 2019c). Implementing the green model of urban land utilization with “low emission, low energy consumption, high growth, and high output” can continuously reduce carbon emissions (Campbell et al. 2012).

The common feature of the above-mentioned literature is that they devote to exploring the relationship between land use and carbon emission system. These studies can provide solid theoretical support for further in-depth analysis of ULUCEI. However, existing studies on ULUCEI need to further explore the following aspects. First, most of these studies mainly focus on urban land use and carbon emissions as two independent systems, and lack of considering them as a whole to reveal their development mechanisms. Second, previous studies are short of revealing the spatiotemporal patterns of China’s ULUCEI. Third, existing studies lack of exploring the evolution trend of ULUCEI. To fill the gap, the contribution of this study mainly concentrates on the following three parts. One is to construct the conceptual framework of ULUCEI and measure the ULUCEI of 334 cities in China from 2000 to 2017. The second one is to analyze the spatiotemporal patterns of China’s ULUCEI by using kernel density estimation (KDE) and exploratory spatial data analysis (ESDA). The third one is to explore the evolution trend by using spatial Markov chains. Through this study, we can obtain a systematical understanding of the current situation of China’s ULUCEI, which is conducive to exploring the practice model of China’s urban land low-carbon utilization. What’s more, China’s practical experiences about ULUCEI can provide valuable references for other developing countries that face the pressure to reduce urban carbon emissions.

Methods and data

Research area

China consists of 34 provinces, with marked differences in economic development, industrial structure, and resource endowments among the provinces. Considering the availability of the data, this paper focuses on 334 cities in the Chinese mainland from 2000 to 2017, in which Hong Kong, Macau, Taiwan, and Tibet are not taken into account. The *Seventh Five-Year Plan for the National Economic and Social Development of*

the People’s Republic of China (NESDC) in 1985 has divided the Chinese mainland into three large regions, namely, eastern, central, and western regions (Fig. 1). This regional classification has been used by many scholars to analyze spatial differences in Chinese economic phenomena (Guan et al. 2018; Liu et al. 2021). In this paper, this regional classification method is used to systematically reveal the spatiotemporal patterns and evolution trend of ULUCEI in China. As shown in Fig. 1, blue, green, and yellow colors identify the eastern, central, and western regions, respectively.

Empirical methods

Research methods adopted in this study mainly include KDE, ESDA, and spatial Markov chains. First, KDE, a nonparametric method, is used to explore the temporal evolution features of China’s ULUCEI. Then, ESDA is proposed to reveal the spatiotemporal patterns of China’s ULUCEI. Moreover, the method of spatial Markov chains is used to analyze the evolution trend of China’s ULUCEI.

Kernel density estimation

Kernel density estimation (KDE) is a popular nonparametric density estimation method (Katkovnik and Shmulevich 2002). This approach uses the kernel density curve to capture the distribution of random variables, which can effectively avoid the subjectivity of function settings in parameter estimation, thereby improving the authenticity of the estimation results (Qin et al. 2011). This advantage has made KDE a typical method for revealing the temporal evolution features (Kuang et al. 2020b). Therefore, this paper describes the evolution characteristics of ULUCEI by observing the position, shape, and ductility of the density function. The principle of KDE is as follows. Assuming that the density function of the random variable X is $f(x)$, the probability density at point x can be expressed by Eq. (1):

$$f(x) = \frac{1}{Nh} \sum_{i=1}^N K\left(\frac{X_i - \bar{x}}{h}\right) \quad (1)$$

In Eq. (1), $K(\cdot)$ is the kernel function; N is the number of observations. h is the bandwidth. X_i is the independent and identically distributed random variable, and \bar{x} is the mean value. The kernel function satisfies $K(x) \geq 0$, $K(x) = K(-x)$, $\int_{-\infty}^{+\infty} K(x)dx = 1$, $\sup K(x) < +\infty$, and $\int_{-\infty}^{+\infty} K^2(x)dx < +\infty$. Generally speaking, h is determined by its relationship with N , and they should satisfy Eq. (2):

$$K(x) = \frac{1}{\sqrt{2\pi}} \exp\left(-\frac{x^2}{2}\right) \quad (2)$$

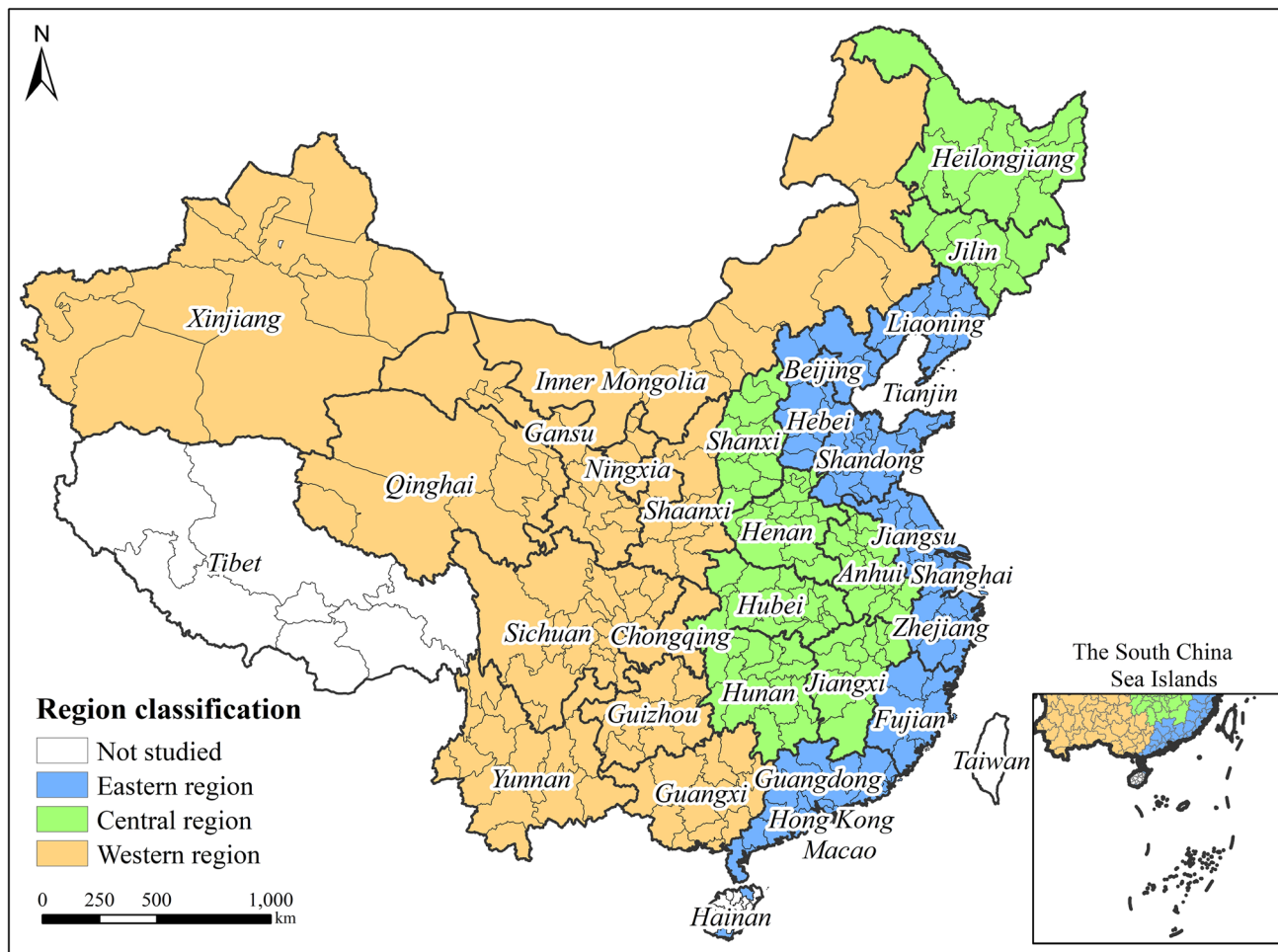


Fig. 1 Research scope and regional classification

Exploratory spatial data analysis

Exploratory spatial data analysis (ESDA) is usually used to describe and visualize the spatial distribution pattern and agglomeration characteristics of attribute values (Kim 2021). This paper uses ESDA to test the spatial patterns of China’s ULUCEI. ESDA includes the global spatial autocorrelation analysis and the local spatial autocorrelation analysis, which can be characterized by global Moran’s *I* and local Moran’s *I*, respectively. Moreover, global Moran’s *I* is used to reveal the overall spatial relationships, and local Moran’s *I* is used to evaluate the local spatial association pattern (Anselin 1995; Anselin et al. 2006). This paper uses ESDA to analyze the spatial patterns of

China’s ULUCEI. The calculation of global Moran’s *I* and local Moran’s *I* can be calculated as follows:

$$I_{global} = \frac{\sum_{i=1}^n \sum_{j=1}^n w_{ij} (x_i - \bar{x})(x_j - \bar{x})}{\sum_{i=1}^n \sum_{j=1}^n w_{ij} (x_i - \bar{x})^2} \tag{3}$$

$$I_{local} = x_i \sum_{j=1}^n w_{ij} x_j \tag{4}$$

where *n* represents the number of sample cities, (*x_i* – \bar{x}) and (*x_j* – \bar{x}) are the deviations of the attribute value and mean value on the city *i* and the city *j*, respectively. *w_{ij}* is

the spatial weight matrix. When the city i and the city j are adjacent, $w_{ij} = 1$. Otherwise, it is 0.

Spatial Markov chains

The method of traditional Markov chains is a Markov process with discrete time and state, which mainly discretizes the continuous data into different types to reveal the probability distribution and evolution trend of each type (Agovino et al. 2019). Accordingly, a $1 \times k$ dimensional matrix $F_t = [F_{1,t}, F_{2,t}, \dots, F_{k,t}]$ is established to store the state probabilities of ULUCEI of each city in year t , and the transition probabilities of ULUCEI in different years can be represented by the $k \times k$ dimensional matrix M (Table 1). According to the principle that the number of each type is similar, this paper divides China’s ULUCEI into four types by using quartile, and their values are divided into A, B, C, and D from small to large. The matrix M is the Markov transition probability matrix; the element P_{ij} indicates the probability of being type i in year t and type j in year $t + 1$. The expression P_{ij} is as follows:

$$P_{ij} = z_{ij} / z_i \tag{5}$$

In Eq. (5), z_{ij} denotes the total number of cities that transferred from type i to type j from year t to year $t + 1$ during the study period. z_i represents the total number of cities belonging to type i in the study period. If the ULUCEI of a city is type i in year t and remains type i in year $t + 1$, the transition type of a city is set as “smooth.” If the ULUCEI of a city increases, the type is set as “upward shift.” Otherwise, it is “downward shift.”

The method of traditional Markov chains mainly focuses on the development of the region itself, while ignoring the adjacent correlation and spatial characteristics of economic phenomena. On the basis of the traditional Markov chains, the method of the spatial Markov chains expresses the domain state of the region by introducing the concept of “spatial lag,” and dynamically reveals the evolution trend of economic phenomena (Le Gallo 2004). By comparing the elements of the traditional Markov transition probability matrix and the spatial Markov transition probability matrix,

Table 1 Traditional Markov transition probability matrix

Type of space	Status at year t	Status at year $(t+1)$			
		A	B	C	D
No lag	A	P_{AA}	P_{AB}	P_{AC}	P_{AD}
	B	P_{BA}	P_{BB}	P_{BC}	P_{BD}
	C	P_{CA}	P_{CB}	P_{CC}	P_{CD}
	D	P_{DA}	P_{DB}	P_{DC}	P_{DD}

we can judge the importance of the regional background to the regional change transition. Therefore, this paper introduces the concept of “spatial lag” as a condition and divides it into k types, decomposes the traditional $k \times k$ dimensional transition probability matrix into the $k \times k \times k$ dimensional transition probability matrix (Table 2), and examines the dynamic evolution of China’s ULUCEI. The element P_{ijk} represents the probability of being type i in year t and type j in the next year under the condition of the spatial lag type k . The spatial lag type considers the units that are geographically adjacent to the city, the spatial lag value Lag_a of city a is the weighted average of the observed value of the geographic units surrounding the city, and its expression is as follows:

$$Lag_a = \sum_{b=1}^n Y_b W_{ab} \tag{6}$$

In Eq. (6), Y_b is the observed value of city b . n is the total number of cities. The spatial weight matrix W_{ab} represents the spatial relationship between city a and city b . This paper uses the adjacency principle to define the spatial relationship.

Indicators and data sources

Indicators used to measure ULUCEI

This paper attempts to propose a conceptual framework for ULUCEI with reference to “urban land use intensity,” which refers to the carbon emissions carried by per unit

Table 2 Spatial Markov transition probability matrix

Spatial lag type	Status at year t	Status at year $(t+1)$			
		A	B	C	D
I	A	P_{AAI}	P_{ABI}	P_{ACI}	P_{ADI}
	B	P_{BAI}	P_{BBI}	P_{BCI}	P_{BDI}
	C	P_{CAI}	P_{CBI}	P_{CCI}	P_{CDI}
	D	P_{DAI}	P_{DBI}	P_{DCI}	P_{DDI}
II	A	P_{AAII}	P_{ABII}	P_{ACII}	P_{ADII}
	B	P_{BAII}	P_{BBII}	P_{BCII}	P_{BDII}
	C	P_{CAII}	P_{CBII}	P_{CCII}	P_{CDII}
	D	P_{DAII}	P_{DBII}	P_{DCII}	P_{DDII}
III	A	P_{AAIII}	P_{ABIII}	P_{ACIII}	P_{ADIII}
	B	P_{BAIII}	P_{BBIII}	P_{BCIII}	P_{BDIII}
	C	P_{CAIII}	P_{CBIII}	P_{CCIII}	P_{CDIII}
	D	P_{DAIII}	P_{DBIII}	P_{DCIII}	P_{DDIII}
IV	A	P_{AAIV}	P_{ABIV}	P_{ACIV}	P_{ADIV}
	B	P_{BAIV}	P_{BBIV}	P_{BCIV}	P_{BDIV}
	C	P_{CAIV}	P_{CBIV}	P_{CCIV}	P_{CDIV}
	D	P_{DAIV}	P_{DBIV}	P_{DCIV}	P_{DDIV}

of urban land area (Huang et al. 2013; Cui et al. 2019). As the spatial carrier of terrestrial ecosystems, urban land use carries carbon emissions generated by urban production and life (Carpio et al. 2021; Zhang et al. 2022). In the process of rapid urbanization, the disorderly expansion and blind construction of urban land have not only caused the loss of carbon storage in urban land (Chuai et al. 2016), but also led to the increase of carbon emissions associated with urban land use (Zhou et al. 2021). Specifically, ULUCEI aims to explore the inherent relationship between urban land use and carbon emissions by measuring the carbon emission carrying the pressure of urban land use, so as to guide the low-carbon use of urban land. Exploring the spatiotemporal patterns and evolution trend of China's ULUCEI is of great value for formulating carbon reduction policies and achieving the "double carbon" targets on schedule. The formula $ULUCEI_{it} = \text{Carbon}_{it} / \text{Land}_{it}$ was used to calculate the value of China's ULUCEI from 2000 to 2017. Where Carbon_{it} represents the total carbon emissions of city i year t , Land_{it} represents the total urban area land of city i year t , $ULUCEI_{it}$ expresses the ULUCEI of city i year t , and the unit is million tons/square kilometer.

Data sources

Taking 334 cities in the Chinese mainland as the research objects, this paper collected the annual statistical data of each city from 2000 to 2017. In fact, there is no official carbon emission data at the city level. Excitingly, the *China Emission Accounts and Datasets* (CEADs) released a set of county-level carbon emissions datasets covering the period 1997 to 2017 (<https://www.ceads.net/data/county/>). These datasets are estimated by unifying the scale of DMSP/OLS and NPP/VIIRS satellite imagery using the particle swarm optimization-back propagation (PSO-BP) algorithm (Chen et al. 2020). In addition, these datasets are considered comprehensive and effective by previous studies (Shan et al. 2021; Liu et al. 2022). Therefore, this paper obtains China's city-level carbon emission data by aggregating county-level carbon emission data in CEADs. The land area data of each city is obtained from the *China Urban Construction Statistical Yearbook* (CUCSY) and *China City Statistical Yearbook* (CCSY).

Results and discussion

Temporal characteristics of ULUCEI

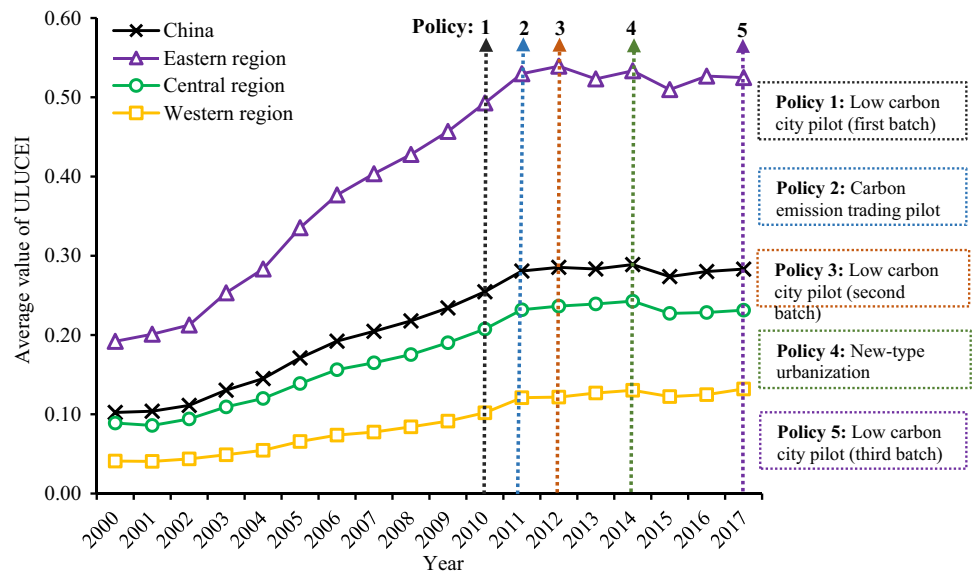
There was an increasing trend of ULUCEI in China and three large regions during the sample period. According

to Fig. 2, China's ULUCEI increased from 0.102 in 2000 to 0.283 in 2017. This temporal feature is closely related to China's urbanization and industrialization trends. In the twenty-first century, China's urbanization and industrialization have entered a stage of rapid development, and the extensive and sprawling urban land development model has occupied a large amount of ecological space, resulting in a rapid increase in carbon emissions (Zhou et al. 2021; Li et al. 2021). From the regional perspective, ULUCEI in China's three large regions showed an upward trend from 2000 to 2017. Specifically, the average value of ULUCEI in the eastern region rose from 0.192 in 2000 to 0.525 in 2017, the central region increased from 0.089 in 2000 to 0.231 in 2017, and the western region increased from 0.041 in 2000 to 0.132 in 2017. Entering the twenty-first century, China's urban population agglomeration, industrial scale expansion, and infrastructure construction promote urban space expansion, which also brings a lot of energy consumption and carbon emissions (Liu and Zhang 2022). Obviously, China's ULUCEI shows a gradually decreasing regional difference from east to west, and the intensity level and growth rate in the eastern region are markedly higher than those in the central and western regions. Eastern cities with developed economies, agglomerated populations, and complete infrastructure have huge advantages in attracting foreign direct investment and large-scale industrial development, which not only stimulate urban spatial expansion but also exacerbate urban carbon emissions. Compared with the east, the cities in the central and western regions are relatively disadvantaged in terms of population size, economic level, and industrial structure, and the carbon emissions of the cities are relatively low.

From the perspective of changing trends, after 2011, China's ULUCEI has changed from rapid improvement to stable development. Actually, this changing trend is closely related to urban carbon reduction policies enacted by the Chinese government. These policies mainly include the three batches of low-carbon city pilots released by the National Development and Reform Commission of the People's Republic of China (NDRC) in 2010, 2012, and 2017 (Zou et al. 2022), the carbon emissions trading pilot in 2011 (Zhang et al. 2021), and the new-type urbanization in 2014 (Sheng and Guo 2016). With the successive implementation of these policies, the transformation of urban industrial structure, optimization of land resource allocation, and enhancement of green technology innovation reduce urban carbon emissions and lead to a gradual stabilization of ULUCEI.

To further reveal the temporal evolution features of China's ULUCEI, this paper adopted the method of KDE to plot kernel density curves of ULUCEI in China and three large regions by using EViews 10.0 software (Fig. 3). From

Fig. 2 Average value of ULUCEI in China and three large regions from 2000 to 2017



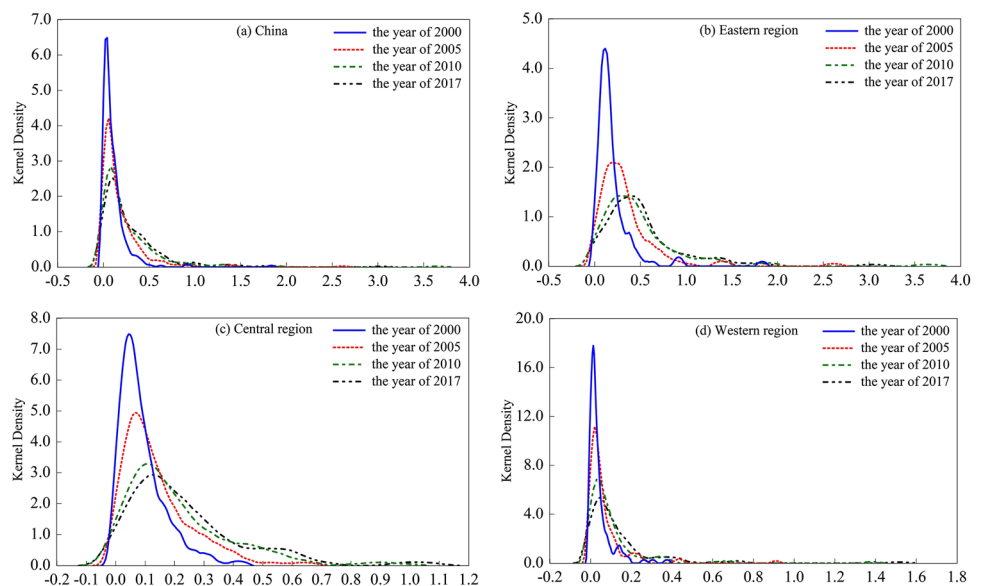
the perspective of the peak height of the curve, China and three large regions showed a gradually decreased trend from 2000 to 2017. From the perspective of the peak position of the curve, China and three large regions shifted to the right from 2000 to 2017. In terms of the number of curve peaks, from 2000 to 2017, China and the central region were dominated by a single peak, and the eastern and western regions changed from “multi-peak” to “single peak.” In terms of the shape of curve peaks, China and the western regions were dominated by “spiky peak,” and the eastern and central regions evolved from “spiky peak” to “broad peak” from 2000 to 2017. In general, the results of KDE indicate that China’s ULUCEI shows an obvious upward and polarized trend. The frequent socio-economic activities such as industrial restructuring, population growth, and urbanization

construction aggravate the transition from carbon sink land to carbon source land (Zhang et al. 2022). Urban carbon emissions have increased significantly, which has led to the reduction in the polarization of ULUCEI.

Spatial pattern of ULUCEI

To visually present the spatial evolution disparities of ULUCEI in China from 2000 to 2017, this paper selected 2000, 2005, 2010, and 2017 as the years of investigation. According to the calculation results of ULUCEI, grading similar values into the same group facilitates comparison. Therefore, this study used the equal interval classification method of ArcGIS, with 0.10 as the equal interval, and China’s ULUCEI is divided into four level groups, namely low

Fig. 3 Kernel density curve of ULUCEI in China and three large regions from 2000 to 2017. Note: this figure is calculated and drawn by using EViews 10.0



intensity ($0 < \text{ULUCEI} \leq 0.10$), medium-low intensity ($0.10 < \text{ULUCEI} \leq 0.20$), medium-high intensity ($0.20 < \text{ULUCEI} \leq 0.30$), and high intensity ($\text{ULUCEI} > 0.30$). As shown in Fig. 4, China's ULUCEI shows an obvious increasing trend, with the number of high-intensity cities increasing nearly sixfold from 21 in 2000 to 121 in 2017. During the study period, there are significant regional differences in the spatial distribution of China's ULUCEI. Low-intensity and medium-low-intensity cities are mainly distributed in the western region. The medium-high-intensity and high-intensity cities are mostly distributed in the eastern region, which are concentrated in the Beijing-Tianjin-Hebei, Yangtze River Delta, Pearl River Delta, and other urban agglomerations. Owing to the large populations, active economies, and developed industries, urban agglomerations have large and concentrated carbon emissions (Cai et al. 2018; Wang et al. 2022), which inevitably leads to a higher level of ULUCEI in these regions.

To reveal the global spatial characteristics of ULUCEI in China, this study conducted spatial autocorrelation tests on ULUCEI in China from 2000 to 2017, and obtained the value of Moran's I and Z statistic (Fig. 5).

The results showed that the values of Moran's I were positive and passed the 1% significance test from 2000 to 2017, indicating that China's ULUCEI showed a positive spatial autocorrelation. The values of Moran's I have experienced a dynamic process from "rapid rise" to "high steady growth," rising from 0.3942 in 2000 to 0.5295 in 2017, indicating that the spatial agglomeration of ULUCEI showed a rapid increase followed by a gradual slowdown. It should be noted that China's urbanization has shown a spatially and geographically concentrated development, gradually forming a regional development pattern dominated by urban agglomerations (Ouyang et al. 2021), promoting the rapid enhancement of the spatial agglomeration of China's ULUCEI. However, with the implementation of policies such as low-carbon city pilots, new-type urbanization construction, and carbon emissions trading pilots, the coordinated development of large, medium, and small cities in China has been advocated (Chen et al. 2018). The ULUCEI of each city has increased significantly, the gap between cities has generally shown a slowing trend, and the spatial agglomeration has gradually stabilized.

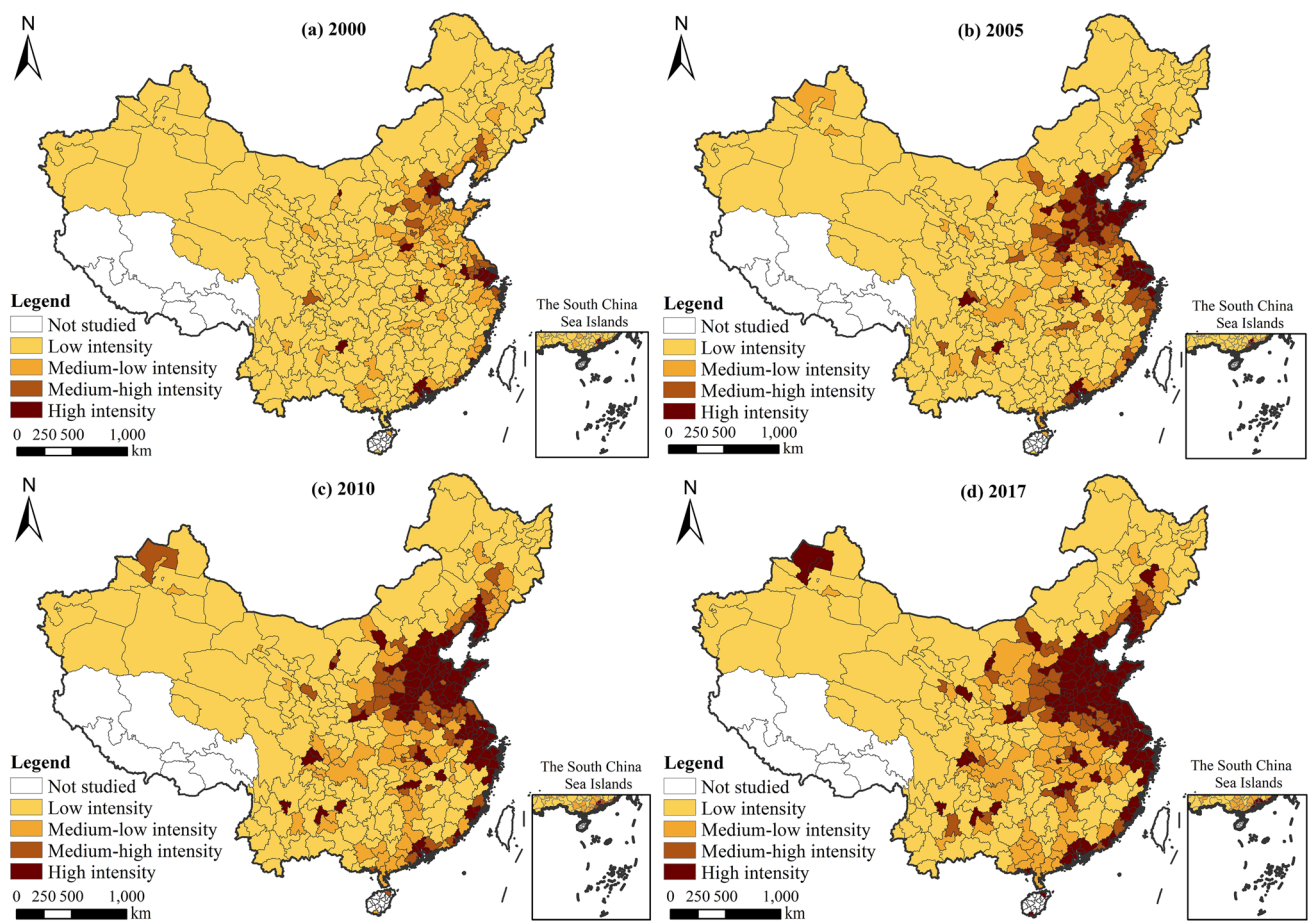
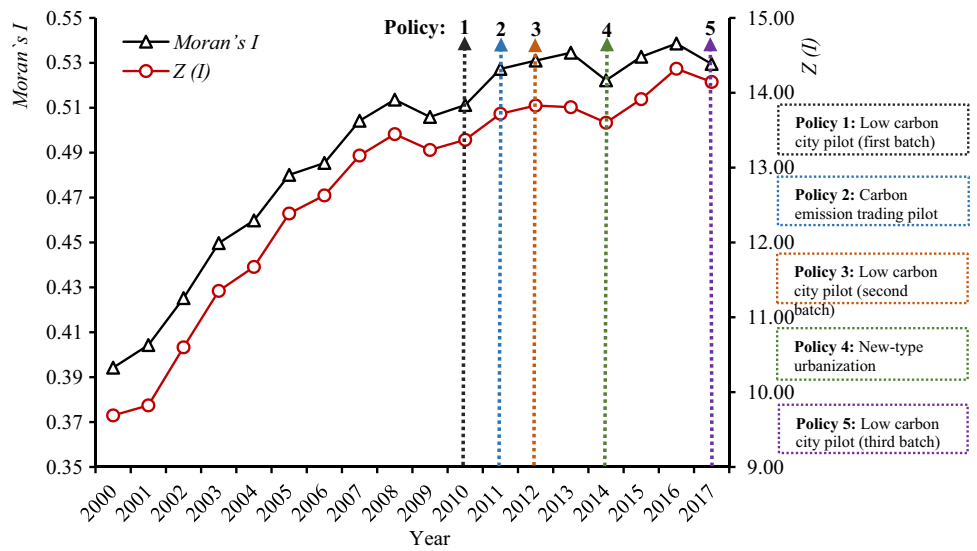


Fig. 4 ULUCEI in China during 2000–2017. Note: this figure is calculated and drawn by using ArcGIS 10.2

Fig. 5 Global Moran's I of ULUCEI in China from 2000 to 2017



To further present the local spatial characteristics of China's ULUCEI, this paper used the LISA (Local Indicators of Spatial Association) cluster maps to divide China's 334 cities into four types (Fig. 6), namely "high-high" agglomeration,

"high-low" polarization, "low-high" collapse, and "low-low" homogeneity. Specifically, "high-high" agglomeration indicates that cities with relatively high ULUCEI are surrounded by cities with also high ULUCEI, showing a significant

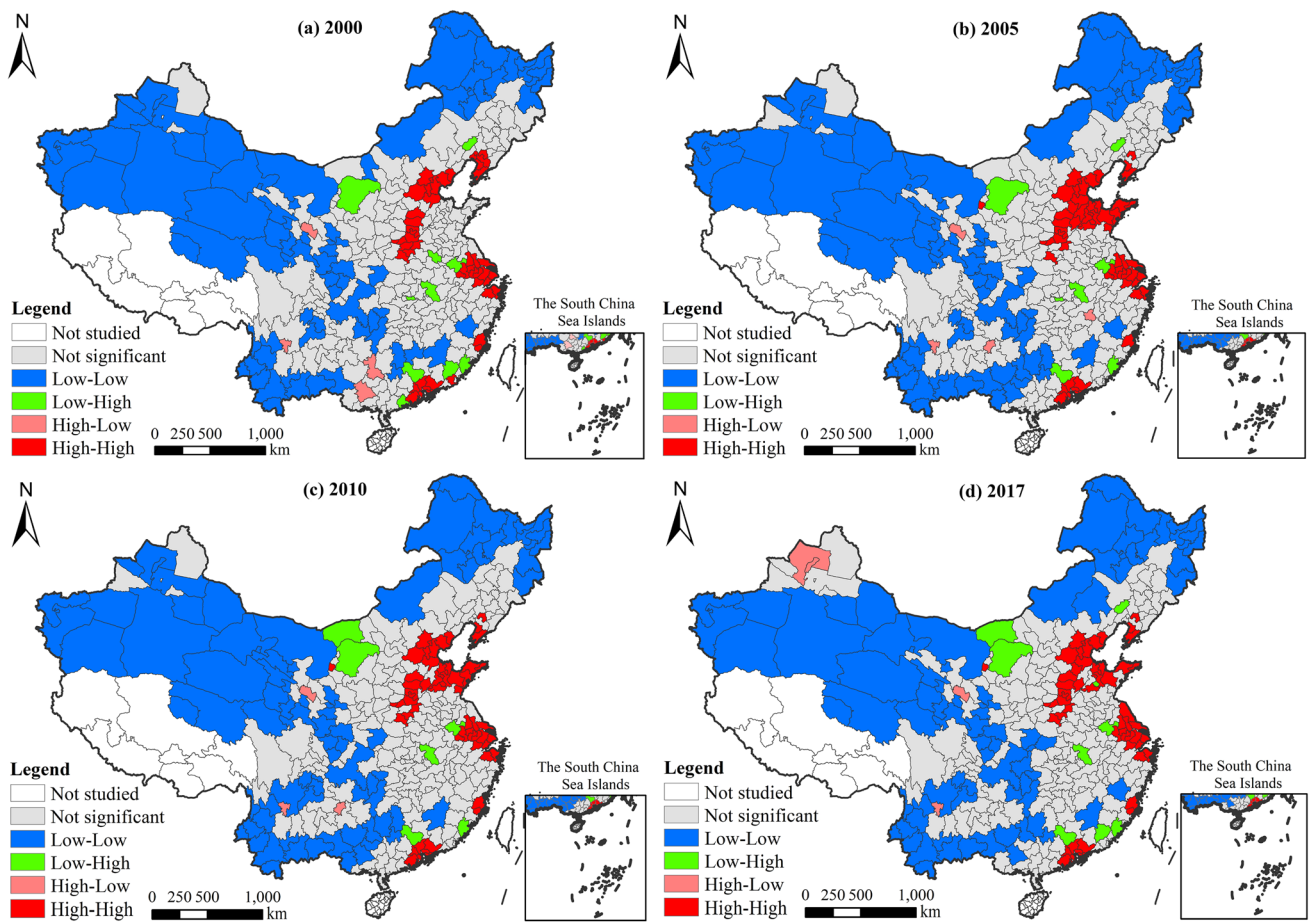


Fig. 6 LISA map of ULUCEI in China during 2000–2017. Note: this figure is calculated and drawn by using GeoDa and ArcGIS 10.2

positive correlation. Cities of this type show an obvious expansion trend and concentrate in urban agglomerations such as Beijing-Tianjin-Hebei, Yangtze River Delta, Pearl River Delta, and Central Plains. “High-low” polarization represents cities with high ULUCEI surrounded by cities with low ULUCEI, showing a significant negative correlation. Cities of this type are mainly scattered in the central and western regions. “Low-high” collapse denotes cities with low ULUCEI surrounded by cities with high ULUCEI, showing a significant negative correlation and remaining relatively stable in spatial distribution and quantity. “Low-low” homogeneity indicates that cities with relatively low ULUCEI are surrounded by cities with also low ULUCEI, showing a significant positive correlation. Cities of this type are mainly distributed in Xinjiang, Inner Mongolia, Yunnan, and other provinces in the western region, presenting a pattern of concentrated contiguous distribution.

Evolution trend of ULUCEI

This study applies the traditional Markov chains to explore the evolution trend of China’s ULUCEI. To be consistent with the above-mentioned content, the quartile method is used to divide China’s ULUCEI into four levels, namely low rank (A), medium-low rank (B), medium-high rank (C), and high rank (D). Subsequently, the transition probability matrix of the traditional Markov chains is obtained (Table 3). From the traditional Markov transition probability matrix, it can be seen that the transition probability of each rank has strong stability. Without the effect of the spatial lag, the probabilities of maintaining steady state for the rank of A, B, C, and D are 93.2%, 90.2%, 90.7%, and 99.3%, respectively. The values on the diagonal are significantly higher than other values in the peer group, indicating that it is relatively difficult to achieve the spatiotemporal transition of China’s ULUCEI. Moreover, the probabilities of transferring upwards range from 6.8 to 9.1%, while the probabilities of shifting downwards range from 0.6 to 1.6%. The probabilities of transferring upwards are significantly higher than that of shifting downwards, which indicates that there is an increasing evolution trend of China’s ULUCEI. Although

Table 3 Traditional Markov transition probability matrix of China’s ULUCEI from 2000 to 2017

Type of space	Status at year <i>t</i>	Status at year (<i>t</i> +1)			
		A	B	C	D
No lag	A	0.932	0.068	0	0
	B	0.006	0.902	0.091	0.001
	C	0	0.016	0.907	0.077
	D	0	0.001	0.006	0.993

there are possibilities of transferring to the adjacent states, the probability of cross-rank transition is smaller.

The “space lag” is added to the Markov transition probability matrix, and four types of space lags are set from low to high, namely *I*, *II*, *III*, and *IV* (Table 4). The results show that the spatial lag affects the transition between cities of different ranks. Under the influence of the spatial lag type *I*, the probabilities of maintaining steady state of ranks A, B, C, and D are 96%, 94.4%, 93.8%, and 100%, respectively. The probabilities of shifting upwards range from 3.9 to 4.9%, while the probabilities of transferring downwards range from 0.7 to 2.3%. When the spatial lag type is *II*, the probabilities of maintaining steady state of ranks A, B, C, and D are 86.7%, 90.7%, 92.6%, and 98.9%, respectively. The probabilities of shifting upwards range from 4.1 to 13.3%, while the probabilities of transferring downwards range from 0.7 to 3.3%. When the spatial lag type is *III*, the probabilities of maintaining steady state of ranks A, B, C, and D are 87.3%, 89%, 92.5%, and 99.2%, respectively. The probabilities of shifting upwards range from 6.9 to 12.7%, while the probabilities of transferring downwards range from 0.5 to 0.8%. When the spatial lag type is *IV*, the probabilities of maintaining steady state of ranks A, B, C, and D are 100%, 68.5%, 83.6%, and 99.3%, respectively. The probabilities of shifting upwards range from 14.1 to 31.5%, while the probabilities of transferring downwards range from 0.7 to 2.3%.

Analyzing the results can be found that the probabilities of maintaining steady state are higher than shifting upwards or transferring downwards, which implied that China’s ULUCEI presents strong stability and “club convergence” trend.

Table 4 Spatial Markov transition probability matrix of China’s ULUCEI from 2000 to 2017

Type of space	Status at year <i>t</i>	Status at year (<i>t</i> +1)			
		A	B	C	D
<i>I</i>	A	0.96	0.04	0	0
	B	0.007	0.944	0.049	0
	C	0	0.023	0.938	0.039
	D	0	0	0	1
<i>II</i>	A	0.867	0.133	0	0
	B	0.007	0.907	0.084	0.001
	C	0	0.033	0.926	0.041
	D	0	0.011	0	0.989
<i>III</i>	A	0.873	0.127	0	0
	B	0.005	0.89	0.105	0
	C	0	0.006	0.925	0.069
	D	0	0	0.008	0.992
<i>IV</i>	A	1	0	0	0
	B	0	0.685	0.315	0
	C	0	0.023	0.836	0.141
	D	0	0	0.007	0.993

The probabilities of shifting upwards are much greater than that of transferring downwards, indicating that China's ULUCEI shows an increasing trend. Moreover, spatial factors significantly affect the dynamic transition of China's ULUCEI, and its effect on the shifting upwards gradually enhances with increasing lag type.

Conclusions and policy implications

Conclusions

This paper constructed a conceptual framework of ULUCEI and measured the ULUCEI of 334 cities in China from 2000 to 2017. On this basis, KDE and ESDA are used to explore the spatiotemporal patterns of China's ULUCEI. Moreover, the method of spatial Markov chains is used to analyze the evolution trend of China's ULUCEI. The main conclusions are as follows:

1. There was an increasing trend of ULUCEI in China and three large regions during the sample period. China's ULUCEI increased from 0.102 in 2000 to 0.283 in 2017. From the regional perspective, the ULUCEI in the eastern region is markedly higher than that in the central and western regions. Specifically, the ULUCEI in the eastern region rose from 0.192 in 2000 to 0.525 in 2017, the central region increased from 0.089 in 2000 to 0.231 in 2017, and the western region increased from 0.041 in 2000 to 0.132 in 2017. After 2012, China's ULUCEI has changed from rapid improvement to stable development. Moreover, the results of nuclear density estimation indicate that China's ULUCEI shows an obvious upward and polarized trend.
2. The spatial distribution of China's ULUCEI has obvious regional differences during the sample period. The results of the global space autocorrelation indicate that China's ULUCEI shows a positive spatial autocorrelation, and the spatial agglomeration shows a rapid increase followed by a gradual slowdown. There are obvious disparities in the distribution rules of cities with different spatial agglomeration forms. Specifically, "High-high" agglomeration cities show an obvious expansion trend and concentrate in urban agglomerations. "High-low" polarization cities are mainly scattered in the central and western regions. The spatial distribution and number of "low-high" collapse cities remain relatively stable. "Low-low" homogeneity cities present a pattern of concentrated contiguous distribution.
3. Without the effect of the spatial lag, the probabilities of remaining stable are higher than 90%, which indicates that it is relatively difficult to achieve the spatiotemporal transition of China's ULUCEI. Under the influence of

the spatial lag, the probabilities of maintaining steady state are still higher than shifting upwards or transferring downwards, which implied that China's ULUCEI presents strong stability and "club convergence" trend. Moreover, spatial factors significantly affect the dynamic transition of China's ULUCEI, and its effect on the shifting upwards gradually enhances with increasing lag type.

Policy implications

According to the main research results obtained in this paper, the following several policy implications for reducing ULUCEI and promoting urban carbon emission reduction in China were proposed.

First, formulating the differentiated urban land low-carbon use models and carbon emission reduction strategies based on the spatiotemporal patterns and evolution trend of China's ULUCEI. The eastern region should exert its technological innovation capabilities and industrial development advantages, improve the economic output of urban land, minimize carbon emissions, and explore new models of low-carbon utilization of urban land. The central region should explore the integration mechanism of industrial development and urban land utilization, improve the regional integrated development model, and promote the coupled development between economic growth and carbon emission reduction. The western region should rely on the national development strategy of western development, promote the close connection between infrastructure construction, industrial development, and low-carbon economy, and improve the potential of urban land low-carbon utilization.

Secondly, transforming the urban land use model to promote urban carbon emission reduction. On the one hand, changing the urban land use mode from "high energy consumption, high emission, and low output" to "low energy consumption, low emission, and high output." On the other hand, exploiting the potential of urban land use, limiting the disorderly expansion of urban space, and reducing carbon emissions caused by urban land expansion.

Finally, optimizing urban spatial layout to promote urban carbon emission reduction. Combining industrial structure upgrading with urban land use planning, strictly limiting energy-intensive, high-emission, and high-pollution industrial land indicators to reduce carbon emissions. Improving the land supply for high-tech industries, reducing urban carbon emissions, and promoting low-carbon use of urban land.

Author contribution Nan Ke: conceptualization; methodology; formal analysis; writing—original draft; data curation. Xinhai Lu: conceptualization; writing—reviewing and editing; resources; supervision; project administration. Xupeng Zhang: data curation, software, validation. Bing Kuang: investigation, funding acquisition, visualization. Yanwei Zhang: methodology, investigation.

Funding This work is supported by the National Natural Science Foundation of China (Nos. 41901256) and the National 985 Project of Non-traditional Security at Huazhong University of Science and Technology.

Data availability The datasets used during the current study are available from the corresponding author on reasonable request.

Declarations

Ethical approval Not applicable.

Consent to participate Not applicable.

Consent for publication Not applicable.

Conflict of interest The authors declare no competing interests.

References

- Agovino M, Crociata A, Sacco PL (2019) Proximity effects in obesity rates in the US: a spatial Markov chains approach. *Soc Sci Med* 220:301–311. <https://doi.org/10.1016/j.socscimed.2018.11.013>
- Ali G, Pumijumnong N, Cui SH (2018) Valuation and validation of carbon sources and sinks through land cover/use change analysis: the case of Bangkok metropolitan area. *Land Use Policy* 70:471–478. <https://doi.org/10.1016/j.landusepol.2017.11.003>
- Andiappan V, Foo DCY, Tan RR (2019) Process-to-Policy (P2Pol): using carbon emission pinch analysis (CEPA) tools for policy-making in the energy sector. *Clean Techn Environ Policy* 21:1383–1388. <https://doi.org/10.1007/s10098-019-01721-0>
- Anselin L (1995) Local indicators of spatial association—LISA. *Geogr Anal* 27(2):93–115. <https://doi.org/10.1111/j.1538-4632.1995.tb00338.x>
- Anselin L, Syabri I, Kho Y (2006) GeoDa: an introduction to spatial data analysis. *Geogr Anal* 38(1):5–22. <https://doi.org/10.1111/j.0016-7363.2005.00671.x>
- Baloch A, Shah SZ, Habibullah MS, Rasheed B (2021) Towards connecting carbon emissions with asymmetric changes in economic growth: evidence from linear and nonlinear ARDL approaches. *Environ Sci Pollut Res* 28(12):15320–15338. <https://doi.org/10.1007/s11356-020-11672-5>
- Bordoloi R, Das B, Tripathi OP, Sahoo UK, Nath AJ, Deb S et al (2022) Satellite based integrated approaches to modelling spatial carbon stock and carbon sequestration potential of different land uses of Northeast India. *Environ Sustain Indic* 13:100166. <https://doi.org/10.1016/j.indic.2021.100166>
- Cai BF, Li WX, Dhakal S, Wang JH (2018) Source data supported high resolution carbon emissions inventory for urban areas of the Beijing-Tianjin-Hebei region: spatial patterns, decomposition and policy implications. *J Environ Manag* 206:786–799. <https://doi.org/10.1016/j.jenvman.2017.11.038>
- Campbell CD, Lilly A, Towers W, Chapman SJ, Werritty A, Hanley N (2012) Land use and a low-carbon society. *Earth Environ Sci Trans R Soc Edinb* 103(2):165–173. <https://doi.org/10.1017/S1755691013000066>
- Carpio A, Ponce-Lopez R, Lozano-García DF (2021) Urban form, land use, and cover change and their impact on carbon emissions in the Monterrey Metropolitan area, Mexico. *Urban Clim* 39:100947. <https://doi.org/10.1016/j.uclim.2021.100947>
- Cen XT, Wu CF, Xing XS, Fang M, Garang ZM, Wu YZ (2015) Coupling intensive land use and landscape ecological security for urban sustainability: an integrated socioeconomic data and spatial metrics analysis in Hangzhou City. *Sustainability* 7(2):1459–1482. <https://doi.org/10.3390/su7021459>
- Chen MX, Liu WD, Lu DD, Chen H, Ye C (2018) Progress of China's new-type urbanization construction since 2014: a preliminary assessment. *Cities* 78:180–193. <https://doi.org/10.1016/j.cities.2018.02.012>
- Chen JD, Gao M, Cheng SL, Hou WX, Song ML, Liu X et al (2020) County-level CO₂ emissions and sequestration in China during 1997–2017. *Sci Data* 7(1):391. <https://doi.org/10.1038/s41597-020-00736-3>
- Chen H, Qi SZ, Tan XJ (2022a) Decomposition and prediction of China's carbon emission intensity towards carbon neutrality: from perspectives of national, regional and sectoral level. *Sci Total Environ* 825:153839. <https://doi.org/10.1016/j.scitotenv.2022.153839>
- Chen BY, Xu C, Wu YY, Li ZW, Song ML, Shen ZY (2022b) Spatiotemporal carbon emissions across the spectrum of Chinese cities: insights from socioeconomic characteristics and ecological capacity. *J Environ Manag* 306:114510. <https://doi.org/10.1016/j.jenvman.2022.114510>
- Chuai XW, Huang XJ, Lu QL, Zhang M, Zhao RQ, Lu JY (2015a) Spatiotemporal changes of built-up land expansion and carbon emissions caused by the Chinese construction industry. *Environ Sci Technol* 49(21):13021–13030. <https://doi.org/10.1021/acs.est.5b01732>
- Chuai XW, Huang XJ, Wang WJ, Zhao RQ, Zhang M, Wu CY (2015b) Land use, total carbon emissions change and low carbon land management in Coastal Jiangsu, China. *J Clean Prod* 103:77–86. <https://doi.org/10.1016/j.jclepro.2014.03.046>
- Chuai XW, Huang XJ, Qi XX, Li JS, Zuo TH, Lu QL et al (2016) A preliminary study of the carbon emissions reduction effects of land use control. *Sci Rep* 6:36901. <https://doi.org/10.1038/srep36901>
- Chuai XW, Yuan Y, Zhang XY, Guo XM, Zhang XL, Xie FJ et al (2019) Multiangle land use-linked carbon balance examination in Nanjing City, China. *Land Use Policy* 84:305–315. <https://doi.org/10.1016/j.landusepol.2019.03.003>
- Cramer W, Guiot J, Fader M, Garrabou J, Gattuso J-P, Iglesias A et al (2018) Climate change and interconnected risks to sustainable development in the Mediterranean. *Nat Clim Chang* 8(11):972–980. <https://doi.org/10.1038/s41558-018-0299-2>
- Cui XL, Wei XQ, Liu W, Zhang F, Li ZH (2019) Spatial and temporal analysis of carbon sources and sinks through land use/cover changes in the Beijing-Tianjin-Hebei urban agglomeration region. *Phys Chem Earth* 110:61–70. <https://doi.org/10.1016/j.pce.2018.10.001>
- Dong F, Li XH, Long RY, Liu X (2013) Regional carbon emission performance in China according to a stochastic frontier model. *Renew Sustain Energy Rev* 28:525–530. <https://doi.org/10.1016/j.rser.2013.08.009>
- Fang CL, Wang SJ, Li GD (2015) Changing urban forms and carbon dioxide emissions in China: a case study of 30 provincial capital cities. *Appl Energy* 158:519–531. <https://doi.org/10.1016/j.apenergy.2015.08.095>
- Feng YJ, Chen SR, Tong XH, Lei ZK, Gao C, Wang JF (2020) Modeling changes in China's 2000–2030 carbon stock caused by land use change. *J Clean Prod* 252:119659. <https://doi.org/10.1016/j.jclepro.2019.119659>
- Grimm NB, Faeth SH, Golubiewski NE, Redman CL, Wu JG, Bai XM et al (2008) Global change and the ecology of cities. *Science* 319:756–760. <https://doi.org/10.1126/science.1150195>
- Guan XL, Wei HK, Lu SS, Su HJ (2018) Mismatch distribution of population and industry in China: pattern, problems and driving factors. *Appl Geogr* 97:61–74. <https://doi.org/10.1016/j.apgeog.2018.05.021>

- He JJ, Zhang PY (2022) Evaluation of carbon emissions associated with land use and cover change in Zhengzhou City of China. *Reg Sustain* 3(1):1–11. <https://doi.org/10.1016/j.regsus.2022.03.002>
- Huang Y, Xia B, Yang L (2013) Relationship study on land use spatial distribution structure and energy-related carbon emission intensity in different land use types of Guangdong, China, 1996–2008. *Sci World J Hindawi Publish Corp* 309680:1–15. <https://doi.org/10.1155/2013/309680>
- Huang B, Hu XP, Fuglstad GA, Zhou X, Zhao WW, Cherubini F (2020) Predominant regional biophysical cooling from recent land cover changes in Europe. *Nat Commun* 11(1):1066. <https://doi.org/10.1038/s41467-020-14890-0>
- Jin G, Guo BS, Deng XZ (2020) Is there a decoupling relationship between CO₂ emission reduction and poverty alleviation in China? *Technol Forecast Soc Change* 151:119856. <https://doi.org/10.1016/j.techfore.2019.119856>
- Jotzo F, Pezzey JCV (2007) Optimal intensity targets for greenhouse gas emissions trading under uncertainty. *Environ Resour Econ* 38(2):259–284. <https://doi.org/10.1007/s10640-006-9078-z>
- Katkovnik V, Shmulevich I (2002) Kernel density estimation with adaptive varying window size. *Pattern Recogn Lett* 23:1641–1648. [https://doi.org/10.1016/S0167-8655\(02\)00127-7](https://doi.org/10.1016/S0167-8655(02)00127-7)
- Kim D (2021) Exploratory study on the spatial relationship between emerging infectious diseases and urban characteristics: Cases from Korea. *Sustain Cities Soc* 66:102672. <https://doi.org/10.1016/j.scs.2020.102672>
- Kuang B, Lu XH, Han J, Fan XY, Zou J (2020a) How urbanization influence urban land consumption intensity: evidence from China. *Habitat Int* 100:102103. <https://doi.org/10.1016/j.habitatint.2019.102103>
- Kuang B, Lu XH, Zhou M, Chen DL (2020b) Provincial cultivated land use efficiency in China: empirical analysis based on the SBM-DEA model with carbon emissions considered. *Technol Forecast Soc Change* 151:119874. <https://doi.org/10.1016/j.techfore.2019.119874>
- Le Gallo J (2004) Space-time analysis of GDP disparities among European regions: a Markov chains approach. *Int Reg Sci Rev* 27(2):138–163. <https://doi.org/10.1177/0160017603262402>
- Li JB, Huang XJ, Kwan MP, Yang H, Chuai XW (2018) The effect of urbanization on carbon dioxide emissions efficiency in the Yangtze River Delta, China. *J Clean Prod* 188:38–48. <https://doi.org/10.1016/j.jclepro.2018.03.198>
- Li JB, Huang XJ, Chuai XW, Yang H (2021) The impact of land urbanization on carbon dioxide emissions in the Yangtze River Delta, China: a multiscale perspective. *Cities* 116:103275. <https://doi.org/10.1016/j.cities.2021.103275>
- Liu G, Zhang F (2022) How do trade-offs between urban expansion and ecological construction influence CO₂ emissions? New evidence from China. *Ecol Indic* 141:109070. <https://doi.org/10.1016/j.ecolind.2022.109070>
- Liu XP, Wang SJ, Wu PJ, Feng KS, Hubacek K, Li X et al (2019) Impacts of urban expansion on terrestrial carbon storage in China. *Environ Sci Technol* 53(12):6834–6844. <https://doi.org/10.1021/acs.est.9b00103>
- Liu XJ, Wang MS, Qiang W, Wu K, Wang XM (2020) Urban form, shrinking cities, and residential carbon emissions: evidence from Chinese city-regions. *Appl Energy* 261:114409. <https://doi.org/10.1016/j.apenergy.2019.114409>
- Liu JG, Li SJ, Ji Q (2021) Regional differences and driving factors analysis of carbon emission intensity from transport sector in China. *Energy* 224:120178. <https://doi.org/10.1016/j.energy.2021.120178>
- Liu QF, Song JP, Dai TQ, Shi A, Xu JH, Wang ER (2022) Spatiotemporal dynamic evolution of carbon emission intensity and the effectiveness of carbon emission reduction at county level based on nighttime light data. *J Clean Prod* 362:132301. <https://doi.org/10.1016/j.jclepro.2022.132301>
- Mendelsohn R, Sohngen B (2019) The net carbon emissions from historic land use and land use change. *J For Econ* 34(3-4):263–283. <https://doi.org/10.1561/112.00000505>
- Neupane PR, Gauli A, Maraseni T, Kübler D, Mundhenk P, Dang MV et al (2017) A segregated assessment of total carbon stocks by the mode of origin and ecological functions of forests: implication on restoration potential. *Int For Rev* 19:120–147. <https://doi.org/10.1505/146554817822330579>
- Normile D (2020) China's bold climate pledge earns praise-but is it feasible? *Science* 370(6512):17–18. <https://doi.org/10.1126/science.370.6512.17>
- Ou JP, Liu XP, Li X, Chen YM (2013) Quantifying the relationship between urban forms and carbon emissions using panel data analysis. *Landsc Ecol* 28(10):1889–1907. <https://doi.org/10.1007/s10980-013-9943-4>
- Ouyang X, Tang LS, Wei X, Li YH (2021) Spatial interaction between urbanization and ecosystem services in Chinese urban agglomerations. *Land Use Policy* 109:105587. <https://doi.org/10.1016/j.landusepol.2021.105587>
- Qin ZL, Li WY, Xiong XF (2011) Estimating wind speed probability distribution using kernel density method. *Electr Power Syst Res* 81(12):2139–2146. <https://doi.org/10.1016/j.epsr.2011.08.009>
- Ribeiro HV, Rybski D, Kropp JP (2019) Effects of changing population or density on urban carbon dioxide emissions. *Nat Commun* 10:3204. <https://doi.org/10.1038/s41467-019-11184-y>
- Ritchie H, Roser M, Rosado P (2020) CO₂ and greenhouse gas emissions. Published online at OurWorldInData.org. <https://ourworldindata.org/co2-and-other-greenhouse-gas-emissions>. Accessed 16 Apr 2022
- Romero-Lankao P, Gurney KR, Seto KC, Chester M, Duren RM, Hughes S et al (2014) A critical knowledge pathway to low-carbon, sustainable futures: integrated understanding of urbanization, urban areas, and carbon. *Earth's Future* 2(10):515–532. <https://doi.org/10.1002/2014EF000258>
- Schuur EAG, McGuire AD, Schadel C, Grosse G, Harden JW, Hayes DJ et al (2015) Climate change and the permafrost carbon feedback. *Nature* 520(7546):171–179. <https://doi.org/10.1038/nature14338>
- Shan YL, Fang S, Cai BF, Zhou Y, Li D, Feng KS et al (2021) Chinese cities exhibit varying degrees of decoupling of economic growth and CO₂ emissions between 2005 and 2015. *One Earth* 4(1):124–134. <https://doi.org/10.1016/j.oneear.2020.12.004>
- Sheng PF, Guo XH (2016) The long-run and short-run impacts of urbanization on carbon dioxide emissions. *Econ Model* 53:208–215. <https://doi.org/10.1016/j.econmod.2015.12.006>
- Shu H, Xiong PP (2019) Reallocation planning of urban industrial land for structure optimization and emission reduction: a practical analysis of urban agglomeration in China's Yangtze River Delta. *Land Use Policy* 81:604–623. <https://doi.org/10.1016/j.landusepol.2018.11.034>
- Simmonds MB, Di Vittorio AV, Jahns C, Johnston E, Jones A, Nico PS (2021) Impacts of California's climate-relevant land use policy scenarios on terrestrial carbon emissions (CO₂ and CH₄) and wildfire risk. *Environ Res Lett* 16(1):014044. <https://doi.org/10.1088/1748-9326/abcc8d>
- Tang MG, Hu FX (2021) How does land urbanization promote CO₂ emissions reduction? Evidence from Chinese prefectural-level cities. *Front Environ Sci* 9:766839. <https://doi.org/10.3389/fenvs.2021.766839>
- Tang XJ, Woodcock CE, Olofsson P, Hutya LR (2021) Spatiotemporal assessment of land use/land cover change and associated carbon emissions and uptake in the Mekong River Basin. *Remote Sens Environ* 256:112336. <https://doi.org/10.1016/j.rse.2021.112336>

- Tian SQ, Wang SJ, Bai XY, Luo GJ, Li Q, Yang YJ et al (2021) Global patterns and changes of carbon emissions from land use during 1992–2015. *Environ Sci Ecotechnol* 7:100108. <https://doi.org/10.1016/j.ese.2021.100108>
- Tollefson J (2016) China's carbon emissions could peak sooner than forecast. *Nature* 531(7595):425–426. <https://doi.org/10.1038/531425a>
- Tong XW, Brandt M, Yue YM, Ciais P, Jepsen MR, Penuelas J et al (2020) Forest management in southern China generates short term extensive carbon sequestration. *Nat Commun* 11(1):129. <https://doi.org/10.1038/s41467-019-13798-8>
- Wang Z, Deng XZ, Bai YP, Chen JC, Zheng WT (2016) Land use structure and emission intensity at regional scale: a case study at the middle reach of the Heihe River basin. *Appl Energy* 183:1581–1593. <https://doi.org/10.1016/j.apenergy.2016.09.109>
- Wang SJ, Zeng JY, Liu XP (2019a) Examining the multiple impacts of technological progress on CO₂ emissions in China: a panel quantile regression approach. *Renew Sust Energ Rev* 103:140–150. <https://doi.org/10.1016/j.jclepro.2018.01.027>
- Wang SJ, Wang JY, Fang CL, Li SJ (2019b) Estimating the impacts of urban form on CO₂ emission efficiency in the Pearl River Delta, China. *Cities* 85:117–129. <https://doi.org/10.1016/j.cities.2018.08.009>
- Wang L, Pei J, Geng J, Niu Z (2019c) Tracking the spatial–temporal evolution of carbon emissions in China from 1999 to 2015: a land use perspective. *Sustainability* 11(17):4531. <https://doi.org/10.3390/su11174531>
- Wang F, Sun XY, Reiner DM, Wu M (2020) Changing trends of the elasticity of China's carbon emission intensity to industry structure and energy efficiency. *Energy Econ* 86:104679. <https://doi.org/10.1016/j.eneco.2020.104679>
- Wang Y, Guo CH, Chen XJ, Jia LQ, Guo XN, Chen RS et al (2021a) Carbon peak and carbon neutrality in China: goals, implementation path and prospects. *China Geol* 4(4):720–746. <https://doi.org/10.31035/cg2021083>
- Wang GZ, Han Q, de Vries B (2021b) The multi-objective spatial optimization of urban land use based on low-carbon city planning. *Ecol Indic* 125:107540. <https://doi.org/10.1016/j.ecolind.2021.107540>
- Wang C, Zhan JY, Zhang F, Liu W, Twumasi-Ankrah MJ (2021c) Analysis of urban carbon balance based on land use dynamics in the Beijing-Tianjin-Hebei region, China. *J Clean Prod* 281:125138. <https://doi.org/10.1016/j.jclepro.2020.125138>
- Wang Y, Niu YJ, Li M, Yu QY, Chen W (2022) Spatial structure and carbon emission of urban agglomerations: spatiotemporal characteristics and driving forces. *Sustain Cities Soc* 78:103600. <https://doi.org/10.1016/j.scs.2021.103600>
- Wu H, Fang SM, Zhang C, Hu SW, Nan D, Yang YY et al (2022) Exploring the impact of urban form on urban land use efficiency under low-carbon emission constraints: a case study in China's Yellow River Basin. *J Environ Manag* 311:114866. <https://doi.org/10.1016/j.jenvman.2022.114866>
- Xia CY, Chen B (2020) Urban land-carbon nexus based on ecological network analysis. *Appl Energy* 276:115465. <https://doi.org/10.1016/j.apenergy.2020.115465>
- Xia CY, Li Y, Xu TB, Chen QX, Ye YM, Shi Z et al (2019) Analyzing spatial patterns of urban carbon metabolism and its response to change of urban size: a case of the Yangtze River Delta, China. *Ecol Indic* 104:615–625. <https://doi.org/10.1016/j.ecolind.2019.05.031>
- Xia CY, Xiang MT, Fang K, Li Y, Ye YM, Shi Z et al (2020) Spatial-temporal distribution of carbon emissions by daily travel and its response to urban form: a case study of Hangzhou, China. *J Clean Prod* 257:120797. <https://doi.org/10.1016/j.jclepro.2020.120797>
- Xu Q, Yang R (2019) The sequential collaborative relationship between economic growth and carbon emissions in the rapid urbanization of the Pearl River Delta. *Environ Sci Pollut Res* 26(29):30130–30144. <https://doi.org/10.1007/s11356-019-06107-9>
- Yang B, Jahanger A, Usman M, Khan MA (2021) The dynamic linkage between globalization, financial development, energy utilization, and environmental sustainability in GCC countries. *Environ Sci Pollut Res* 28:16568–16588. <https://doi.org/10.1007/s11356-020-11576-4>
- Zhang RS, Matsushima K, Kobayashi K (2018) Can land use planning help mitigate transport-related carbon emissions? A case of Changzhou. *Land Use Policy* 74:32–40. <https://doi.org/10.1016/j.landusepol.2017.04.025>
- Zhang XM, Lu FF, Xue D (2021) Does China's carbon emission trading policy improve regional energy efficiency? -an analysis based on quasi-experimental and policy spillover effects. *Environ Sci Pollut Res* 29(14):21166–21183. <https://doi.org/10.1007/s11356-021-17021-4>
- Zhang CY, Zhao L, Zhang HT, Chen MN, Fang RY, Yao Y et al (2022) Spatial-temporal characteristics of carbon emissions from land use change in Yellow River Delta region, China. *Ecol Indic* 136:108623. <https://doi.org/10.1016/j.ecolind.2022.108623>
- Zhou Y, Chen MX, Tang ZP, Mei ZA (2021) Urbanization, land use change, and carbon emissions: quantitative assessments for city-level carbon emissions in Beijing-Tianjin-Hebei region. *Sustain Cities Soc* 66:102701. <https://doi.org/10.1016/j.scs.2020.102701>
- Zhu EY, Deng JS, Zhou MM, Gan M, Jiang RW, Wang K et al (2019) Carbon emissions induced by land-use and land-cover change from 1970 to 2010 in Zhejiang, China. *Sci Total Environ* 646:930–939. <https://doi.org/10.1016/j.scitotenv.2018.07.317>
- Zou C, Huang YC, Wu SS, Hu SL (2022) Does “low-carbon city” accelerate urban innovation? Evidence from China. *Sustain Cities Soc* 83:103954. <https://doi.org/10.1016/j.scs.2022.103954>

Publisher's note Springer Nature remains neutral with regard to jurisdictional claims in published maps and institutional affiliations.

Springer Nature or its licensor holds exclusive rights to this article under a publishing agreement with the author(s) or other rightsholder(s); author self-archiving of the accepted manuscript version of this article is solely governed by the terms of such publishing agreement and applicable law.